Journal of Applied Electrochemistry **31**: 455–460, 2001.

Corrosion behaviour of Ti–4Al–4V alloy in nitric, phosphoric and sulfuric acid solutions at room temperature

A. ROBIN, J.L. ROSA and H.R.Z. SANDIM
Departamento de Engenharia de Materiais – Faculdade de Engenharia Química de Lorena, Caixa Postal 116, 12600-000 Lorena, SP, Brazil

Received 22 December 1999; accepted in revised form 17 October 2000

Key words: corrosion, nitric acid, phosphoric acid, sulfuric acid, Ti–Al–V alloy

Abstract

Electron beam melting of Ti-6-4 scrap has been carried out. Aluminium losses were verified for all the runs and commercial-size ingots of Ti-4-4 alloy were obtained. Tensile tests and hardness measurements have shown that the Ti-4-4 alloy has mechanical strength close to the Ti-6-4 alloy as well as higher ductility. The corrosion behaviour of the Ti-4-4 alloy was investigated in HNO_3, H_3PO_4 and H_2SO_4 solutions at room temperature. Ti-4-4 alloy is passive in all HNO_3 solutions and in 20 wt % H_3PO_4 and presents an active behaviour in 40–80 wt % H_3PO_4 and in all H_2SO_4 solutions. Ti-4-4 alloy is highly corrosion resistant in HNO_3 and 20 wt % H_3PO_4 and has a moderate resistance in 40 wt % H_3PO_4. Ti-4-4 alloy can be regarded as a potential candidate to replace CP–Ti in these media. In more concentrated H_3PO_4 solutions, and in H_2SO_4, very high corrosion rates were observed.

1. Introduction

Ti–6%Al–4%V (Ti-6-4) is widely used in the aerospace and aircraft industries for the manufacture of high-strength components because titanium saves weight in highly loaded structures operating at low-to-moderate elevated temperatures [1]. Owing to the rigorous specifications required for the fabrication of these parts, large amounts of Ti-6-4 (scrap) are available for recycling [2].

To verify the properties of the alloy produced after electron beam melting (EBM) of the Ti-6-4, several melting tests were carried out [3]. An expected depletion of the aluminium content was observed, leading to the production of an alloy with nominal composition close to Ti–4%Al–4%V (Ti-4-4).

The use of this alloy as a possible substitute for commercially-pure titanium (CP–Ti) in chemical engineering applications, including cast parts, is promising because of the low cost of the scrap and the similarity of its microstructure and mechanical properties to that of Ti-6-4.

Pure titanium offers outstanding corrosion resistance in a wide variety of environments, specially oxidizing, neutral and inhibited reducing media [4, 5]. The corrosion resistance of titanium is due to the formation of a protective and self adherent oxide film [4, 6]. For this reason, titanium is widely used for handling nitric acid in industrial applications (valves, storage tanks and thermometric devices) and marine environments. The presence of oxidizing species, such as oxygen, ferric, cupric and chromic ions, improves the performance of titanium [7–9].

Much work has been published in the last two decades on the corrosion and passivation of titanium and Ti–Al–V alloys. Most papers deal with the study the passive film characteristics [10–17], stress–corrosion cracking in acidic methanol [18–20], effect of ion implantation [21–23], behaviour in physiological environment for implant applications [24–28] and influence of inhibitors in acid media [29–32]. Frayret [33–34] studied the anodic behaviour of titanium, Ti–Al, Ti–V and Ti–Al–V alloys in HCl and proposed a model to explain dissolution and passivation. The influence of acid concentration and/or temperature on corrosion behaviour was examined for titanium in HCl [35], H_2SO_4 [36] and H_3PO_4 [37] and for Ti–6Al–4V in H_3PO_4 [38].

The purpose of this paper is to study the electrochemical behaviour of Ti-4-4 alloy in three widely used mineral acids HNO_3, H_3PO_4, and H_2SO_4 at room temperature. This investigation is based on open-circuit and potentiodynamic measurements. The results are compared with data obtained on CP–Ti under the same conditions.

2. Experimental procedure

2.1. *Materials*

Ti-6-4 scrap was melted in a 300 kW electron beam furnace (ES-2/18/300, Leybold-Heraeus) using a water-cooled copper crucible (100 or 150 mm dia.)

Table 1. Chemical composition of CP–Ti, Ti-6-4 and Ti-4-4 alloys

Materials	C /wt ppm	O /wt ppm	N /wt ppm	Fe /wt ppm	Al /wt %	V /wt %
CP–Ti	< 100	< 400	< 100	< 300	–	–
Ti-6-4	< 800	< 2000	< 500	< 3000	6.25 ± 0.5	4.0 ± 0.5
Ti-4-4	< 800	< 2000	< 500	< 2000	4.50 ± 0.5	3.9 ± 0.3

under high vacuum ($< 10^{-3}$ Pa). Low-iron titanium sponge was pressed into briquettes and melted under the same conditions as above mentioned. Electron beam melting of Ti-6-4 alloy leads to an aluminium-depleted material with nominal composition close to Ti–4% Al–4%V (Ti-4-4). Chemical composition was determined in an inductively coupled plasma spectrophotometer (model 3410, ARL). Gas analyses were carried out by means of sample melting and inert gas carrier technique (TC-136, Leco Co.). The chemical composition of Ti-6-4 scrap and CP–Ti and Ti-4-4 ingots is shown in Table 1.

The microstructure of the Ti-4-4 alloy in the 'as-cast' condition is characterized by the presence of a coarse plate-like Widmanstätten structure and the occurrence of α-phase at the grain boundaries (Figure 1). There is no appreciable difference between the microstructures of Ti-6-4 and Ti-4-4 'as-cast' alloys.

To determine the mechanical properties of the materials investigated, tensile tests were performed according to the ASTM-E8-84 standard [39]. Specimens were cut out from hot swaged (900 °C) CP–Ti and Ti-4-4 bars after 90% of reduction in area and from 'as-received' Ti-6-4 bars. The results of tensile tests and Vickers hardness measurements are presented in Table 2. The recycled alloy presents a similar mechanical strength and a higher ductility when compared to Ti-6-4.

2.2. *Electrochemical study*

CP–Ti and Ti-4-4 specimens were prepared from transverse slices (100 mm dia. × 10 mm thick) cut from the electron beam melted ingots. Cylindrical tests specimens

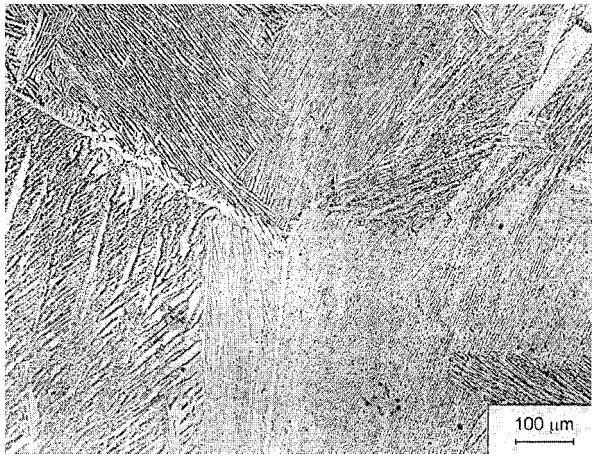

Fig. 1. Microstructure of Ti-4-4 alloy ingot.

Table 2. Mechanical properties of CP–Ti, Ti-6-4 (as received) and Ti-4-4 alloys

Material	CP–Ti	Ti-6-4	Ti-4-4
Yield strength/MPa	259 ± 59	875 ± 18	863 ± 93
Ultimate tensile strength/MPa	373 ± 50	994 ± 13	958 ± 69
Ultimate elongation/%	> 40	5.1 ± 1.7	21.0 ± 5.9
Reduction in area/%	87.6 ± 1.7	28.5 ± 3.0	47.0 ± 4.6
Vickers hardness/HV-10	130 ± 10	340 ± 7	347 ± 14

(8 mm dia. × 15 mm length) were obtained from these slices and mounted in PTFE holders. The cross section of the electrodes (0.5 cm^2 area) was mechanically ground with emery-paper up to 600 grit, degreased with acetone, rinsed with distilled water and dried with air.

The solutions, prepared from analytical reagents and deionized water, were 20–40–60 wt % HNO_3, 20–40–60–80 wt % H_3PO_4 and 20–40–60–80 wt % H_2SO_4. The solutions were naturally aerated and no stirring was operated during the tests. The temperature of the solutions was maintained at 25 ± 2 °C. The counter electrode was a square-shaped platinum sheet of 18 cm^2 area. All potentials were referred to the saturated calomel electrode (SCE) potential (0.242 V vs SHE).

The electrochemical experiments were performed using a PAR 273A potentiostat controlled with a microcomputer through M352 Corrosion Software.

Prior to cathodic and/or anodic polarization, the working electrodes were immersed in the solutions for nearly 3 h for stabilization of the open-circuit potential. The polarization studies were carried out potentiodynamically with a 0.1 mV s^{-1} potential sweep rate. After each polarization experiment, the samples were reground with emery paper to a 600 grit finish in order to remove any product formed on the metal surface which could affect the following tests, rinsed with deionized water and dried.

Some immersion tests of Ti-4-4 rectangular coupons (30 mm × 20 mm × 3 mm) were carried out in HNO_3, H_3PO_4 and H_2SO_4 for 163 h. The solutions were analysed by inductively coupled plasma spectrophotometry in order to determine the Ti, Al and V contents.

3. Results and discussion

3.1. *Corrosion behaviour in HNO_3 solutions*

Figure 2(a) shows the variation in open-circuit potential of Ti-4-4 alloy in 20, 40 and 60 wt % HNO_3 solutions at room temperature as a function of exposure time. The potentials drift in the positive direction with time for the three acid concentrations and tend to stabilize around an average value for long exposure times. This shift is associated with thickening of the oxide film formed on the material surface. The corrosion potentials stabilize when the rate of film formation equals the rate of film dissolution. A shift in potential to more noble values occurs as the acid concentration increases, showing the

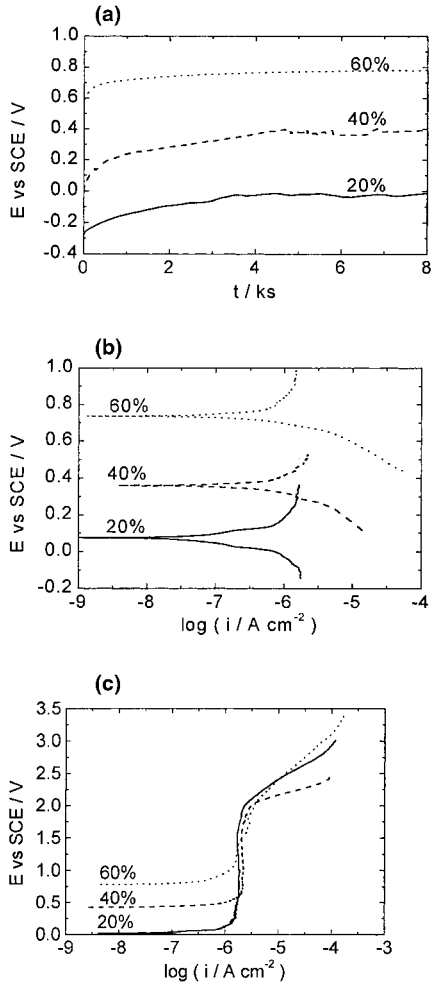

Fig. 2. (a) Variation of the open-circuit potential with time, (b) anodic and cathodic polarization curves and (c) anodic polarization curves for Ti-4-4 alloy in 20, 40 and 60 wt % HNO_3 solutions at room temperature.

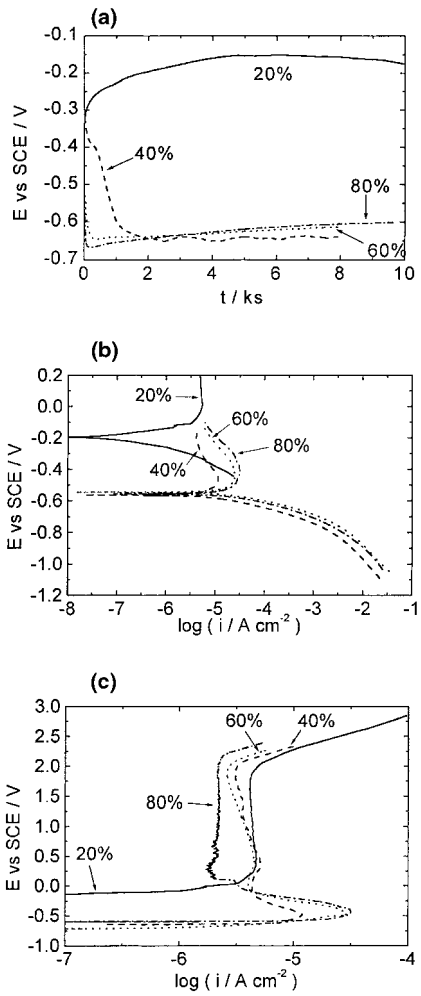

Fig. 3. (a) Variation of the open-circuit potential with time, (b) anodic and cathodic polarization curves and (c) anodic polarization curves for Ti-4-4 alloy in 20, 40, 60 and 80 wt % H_3PO_4 solutions at room temperature.

oxidizing character of HNO_3. All the corrosion potentials are in the TiO_2 stability region of the Ti–H_2O Pourbaix diagram [40].

The cathodic and anodic polarization curves are presented in Figure 2(b). The corrosion current densities tend to increase slightly with acid concentration. All the corrosion rates are around 25 μm per year. These values were deduced from the corrosion current densities and Faraday's law considering titanium to be dissolved to the trivalent oxidation state. These low values show that this alloy is able to handle HNO_3 solutions at room temperature as CP–Ti does.

Figure 2(c) shows the anodic polarization curves for Ti-4-4 alloy in the HNO_3 solutions. No active–passive transition is observed which shows that the Ti-4-4 alloy is spontaneously passive in HNO_3 at room temperature. From these curves, the current densities are almost constant in the passive region for 20 and 40 wt % HNO_3 but increase continuously for 60 wt % HNO_3 as the potential increases. The passive current densities do not vary significantly with HNO_3 concentration. Above nearly 2 V vs SCE, the anodic current densities increase significantly due to oxygen evolution.

3.2. *Corrosion behaviour in H_3PO_4 solutions*

The open-circuit potential versus time curves of the Ti-4-4 alloy in 20–80 wt % H_3PO_4 solutions are presented in Figure 3(a). Two different types of behaviour are observed. In 20 wt % H_3PO_4, the potential drifts to more noble values with time and tends to stabilize at long exposure times. For 40 to 80 wt % H_3PO_4, the potentials shift in the active direction with time and reach a steady state for long exposure times. The positive shift in potential is associated with oxide film thickening. In contrast, the negative shift is related to film dissolution and the consecutive active dissolution of the base metal. The potential measured for 20 wt % H_3PO_4 solutions lies in the passive region on the Ti–H_2O Pourbaix diagram, whereas the potentials obtained for 40 to 80 wt % H_3PO_4 are in the active region [40]. No notable difference in the steady state corrosion potentials can be detected when the acid concentration increases from 40 to 80 wt % H_3PO_4.

Anodic and cathodic polarization curves of the Ti-4-4 alloy are shown in Figure 3(b). The corrosion and

critical current densities increase with increasing acid concentrations in the 40–80 wt % H_3PO_4 range. The corrosion current density is lower in 20 wt % H_3PO_4 solution. Using Faraday's law, corrosion rates of 8, 257, 870 and 1056 μm per year are calculated in 20, 40, 60 and 80 wt % H_3PO_4, respectively.

Figure 3(c) shows the anodic polarization curves obtained for the Ti-4-4 alloy in 20–80 wt % H_3PO_4 solutions. The Ti-4-4 alloy is passive in 20 wt % H_3PO_4 since an active–passive transition is not observed. At higher concentrations this transition clearly appears. Singh and Hosseini [38] investigated the behaviour of the Ti-6-4 alloy in deaerated 1 to 13 M H_3PO_4 solutions, but did not observe spontaneous passivity in low concentrated solutions, like 1 M (~11 wt %) and 3 M (~25 wt %) H_3PO_4. They observed, for all H_3PO_4 concentrations, a spontaneous active dissolution and an active–passive transition during anodic polarization. The difference between these results in 1 and 3 M H_3PO_4 and ours in 20 wt % H_3PO_4 may be due to the fact we used naturally aerated solutions, which might tend to enhance the passivity in low concentrated acid solutions. Our passive current densities decrease slightly with an increasing acid concentration. As observed in HNO_3 solutions, the anodic current density increases above 2 V vs SCE due to oxygen evolution.

3.3. *Corrosion behaviour in H_2SO_4 solutions*

The evolution of open-circuit potentials with time for the Ti-4-4 alloy in 20–80 wt % H_2SO_4 solutions is shown in Figure 4(a). All potentials shift in the negative direction and reach steady-state values for long exposure times. The stabilized potentials for all acid concentrations are in the active region of the Pourbaix diagram [40]. This behaviour demonstrates the active dissolution of the material in H_2SO_4 solutions at room temperature. The stabilized corrosion potentials become more active as the H_2SO_4 concentration increases from 20 to 60 wt % H_2SO_4 but shift to less negative values in 80 wt % H_2SO_4.

The values of the corrosion current densities measured from the cathodic polarization curves increase with increasing acid concentration (Figure 4(b)). The corrosion rates calculated from Faraday's law are higher than 1.5 mm per year showing that Ti-4-4 alloy is unable to be used as a corrosion-resistant material in H_2SO_4 solutions.

The anodic polarization curves obtained for all acid concentrations display an active–passive transition and a passive region up to 2 V vs SCE, where oxygen evolution commences (Figure 4(c)). The critical and passive current densities of the Ti-4-4 alloy increase with increasing acid concentration.

Similar behaviour was observed for CP–Ti in HNO_3, H_3PO_4 and H_2SO_4 solutions at room temperature. The corrosion potentials of CP–Ti measured in the various acid solutions show that CP–Ti is spontaneously passive in HNO_3 solutions and in 20 wt % H_3PO_4 and has

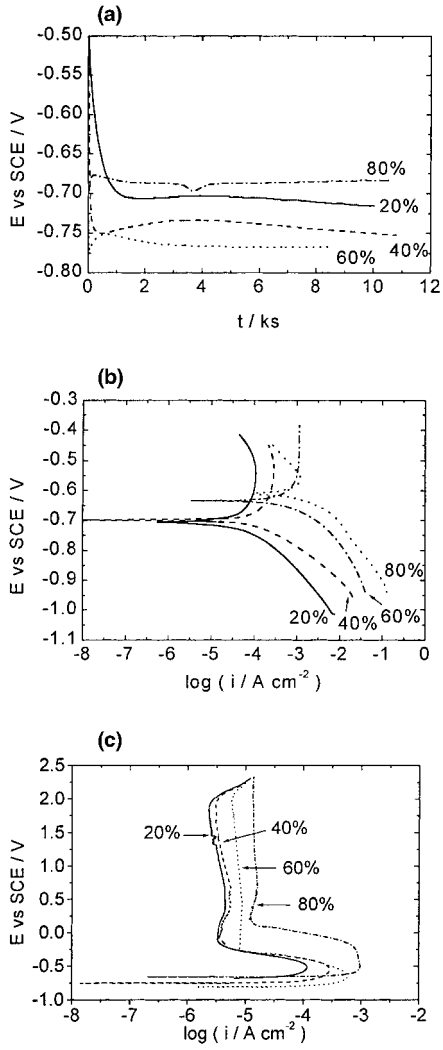

Fig. 4. (a) Variation of the open-circuit potential with time, (b) anodic and cathodic polarization curves and (c) anodic polarization curves for Ti-4-4 alloy in 20, 40, 60 and 80 wt % H_2SO_4 solutions at room temperature.

active behaviour in 40–80 wt % H_3PO_4 and all H_2SO_4 solutions (Table 3). The values of corrosion, critical and passive current densities show that Ti–CP tends to be slightly more corrosion resistant than Ti-4-4 alloy (Tables 4, 5 and 6).

The Ti-4-4 samples after immersion in HNO_3 and 20 wt % H_3PO_4 had a yellowish surface, whereas those tested in H_2SO_4 and 40–80 wt % H_3PO_4 had a silvery and etched surface. These observations are in accordance with the electrochemical study: passivation of the alloy in the first solutions and active dissolution in the lattest ones.

The relative amounts of Ti, Al and V in solutions after immersion tests are summarized in Table 7. In H_2SO_4 and 40 to 80 wt % H_3PO_4 solutions, where spontaneous active dissolution takes place, the relative amounts of the elements are similar to the corresponding values in the Ti-4-4 alloy, indicating that no selective dissolution occurred. In contrast, the relative element amounts in the other solutions, where the alloy is spontaneously passive, differ significantly from those of the alloy. Some

Table 3. Corrosion potentials of Ti-4-4 alloy and CP–Ti in acid solutions at room temperature

Acid concentration/wt %		Corrosion potential vs SCE/mV	
		Ti-4-4	CP–Ti
HNO_3	20	−37	−19
	40	402	443
	60	785	777
H_3PO_4	20	−171	−166
	40	−643	−651
	60	−612	−554
	80	−601	−560
H_2SO_4	20	−716	−677
	40	−752	−742
	60	−766	−754
	80	−683	−687

causes can be suggested: (i) the element contents in the passive film may be different from the base alloy and the chemical composition of this film may vary with the solution composition, (ii) assuming that the passive film has the same metallic composition than the alloy, a preferential dissolution of Al from the passive film may occur.

The corrosion rates deduced from the Ti, Al and V concentrations in HNO_3, 20–40 wt % H_3PO_4 and 20–40 wt % H_2SO_4 are in accordance with the values obtained from the potentiodynamic study. In 60–80 wt % H_3PO_4 and 60–80 wt % H_2SO_4, much smaller corrosion rates were calculated from the immersion tests. Such a result may be due to the Ti ions dissolved in solutions during the corrosion process, which can act, if in sufficient amount, as inhibitors of the corrosion process [41].

Table 4. Corrosion current densities of Ti-4-4 alloy and CP–Ti in acid solutions at room temperature

Acid concentration/wt %		Current density/μA cm^{-2}	
		Ti-4-4	CP–Ti
HNO_3	20	1.6	1.5
	40	2.0	1.3
	60	2.1	2.3
H_3PO_4	20	0.7	0.8
	40	22.2	31.7
	60	75.1	47.0
	80	91.3	52.5
H_2SO_4	20	141	166
	40	158	223
	60	3010	1210
	80	4560	6860

Table 5. Critical current densities of Ti-4-4 alloy and CP–Ti in acid solutions at room temperature

Acid concentration/wt %		Current density/μA cm^{-2}	
		Ti-4-4	CP–Ti
H_3PO_4	40	12.0	13.5
	60	23.7	21.4
	80	31.4	26.7
H_2SO_4	20	108	100
	40	316	457
	60	631	–
	80	1200	1040

Table 6. Passive current densities of Ti-4-4 alloy and CP–Ti in acid solutions at room temperature

Acid concentration/wt %		Current density/μA cm^{-2}	
		Ti-4-4	CP–Ti
HNO_3	20	1.7	1.9
	40	2.1	2.3
	60	1.8	–
H_3PO_4	20	4.3	3.6
	40	3.5	3.6
	60	3.4	2.3
	80	2.5	2.1
H_2SO_4	20	2.5	2.7
	40	3.4	4.0
	60	7.9	–
	80	11.4	14.3

Table 7. Relative amounts of Ti, Al and V (in %) in the acid solutions after 163 h immersion tests

Acid solution		Element		
		Ti	Al	V
HNO_3	20%	45	53	2
	40%	39	59	2
	60%	28	70	2
H_3PO_4	20%	65	33	2
H_3PO_4 and H_2SO_4	40–80% 20–80%	90–92	4–7	3–4

4. Conclusions

The Ti-4-4 alloy obtained by electron beam melting of Ti-6-4 scrap has mechanical strength close to the Ti-6-4 alloy as well as higher ductility.

The study of Ti-4-4 corrosion behaviour in HNO_3, H_3PO_4 and H_2SO_4 solutions at room temperature shows that:

(i) Ti-4-4 alloy is passive in all HNO_3 solutions and in 20 wt % H_3PO_4.
(ii) Ti-4-4 alloy has active behaviour in 40–80 wt % H_3PO_4 and in all H_2SO_4 solutions.
(iii) Ti-4-4 alloy has a high corrosion resistance in HNO_3 and 20 wt % H_3PO_4, a moderate resistance in 40 wt % H_3PO_4 and can be regarded as a potential candidate to replace CP–Ti for the manufacture of corrosion-resistant equipments operating in these media.
(iv) In 60 and 80 wt % H_3PO_4 and in H_2SO_4 solutions, very high corrosion rates were measured.

References

1. M.J. Donachie Jr., 'Titanium: A Technical Guide', ASM International, Metals Park, OH, (1988).
2. C.E. Nelson, Advances in cost effective processing of titanium, *in* Proceedings of Paris Conference on 'Synthesis, Processing and Modelling of Advanced Materials', ASM, Paris (1991), p. 157.
3. H.R.Z. Sandim, C.A.R.P. Baptista, M.J.R. Barbosa and C.A. Nunes, Reciclagem da Liga Ti–6%Al–4%V via Fusão por Feixe Eletrônico, *in* Anais do VIII Seminário de Metais Não-Ferrosos, ABM, São Paulo (1993), p. 71.
4. L.R. Covington and R.W. Schutz, 'Corrosion Resistance of Titanium', Timet Division/TMCA Brochure (not dated).
5. B.D. Craig and D.S. Anderson, 'Handbook of Corrosion Data', (ASM International, Metals Park, OH, 1995).
6. R.W. Schutz and L.C. Covington, *Corrosion* **37** (1981) 585.
7. H.B. Bomberger, Factors which influence corrosion properties of titanium, *in* 'Industrial Applications of Ti and Zr', Third Conference, ASTM (1984), p. 143.
8. L.C. Covington and R.W. Schutz, Effects of iron on the corrosion resistance of titanium, *in* E.W. Kleefisch (Ed), 'Industrial Applications of Titanium and Zirconium', ASTM STP 728 (1981), p. 163
9. T. Fijii and H. Baba, *Corros. Sci.* **31** (1990) 275.
10. M.S. El-Basiouny and A.A. Mazhar, *Corrosion* **38** (1982) 237.
11. M.M. Hefny, A.G. Gad-Allah, S.A. Salih and M.S. El-Basiouny, *Corrosion* **40** (1984) 245.
12. A.G. Gad-Allah, A.A. Mazhar and M.S. El-Basiouny, *Corrosion* **42** (1986) 740.
13. A.A. Mazhar, F.E. Heakal and A.G. Gad-Allah, *Corrosion* **44** (1988) 705.
14. A.G. Gad-Allah and A.A. Mazhar, *Corrosion* **46** (1990) 306.
15. W.A. Badawy, *Indian J. Technol.* **29** (1991) 235.
16. W.A. Badawy, S.S. Elegamy and Kh.M. Ismail, *Br. Corros. J.* **28** (1993) 133.
17. S.Y. Yu, C.W. Brodrick, M.P. Ryan and J.R. Scully, *J. Electrochem. Soc.* **146** (1999) 4429.
18. X.G. Zhang and J. Vereecken, *Corrosion* **45** (1989) 57.
19. X.G. Zhang and J. Vereecken, *Corrosion* **46** (1990) 136.
20. D.J. Simbi and J.C. Scully, *Corrosion* **53** (1997) 298.
21. H. Schmidt and H.E. Exner, *Z. Met.* **90** (1999) 594.
22. T. Sundararajan, U.K. Mudali, K.G.M. Nair, S. Rajeswari and M. Subbaiyan, *Werkst. Korros.* **50** (1999) 344.
23. J. Baszkiewicz, M. Kamiinski, J. Kozubowski, D. Krupa, K. Gosiewska, A. Barcz, G. Gawlik and J. Jagielski, *J. Mater. Sci.* **35** (2000) 767.
24. Y. Okazaki, Y. Ito, K. Kyo and T. Tateishi, *Mater. Sci. Eng. A* **213** (1996) 138.
25. J. Pan, D. Thierry and C. Leygraf, *Electrochim. Acta* **41** (1996) 1143.
26. M. Nakagawa, S. Matsuya, T. Shiraishi and M. Ohta, *J. Dental Res.* **78** (1999) 1568.
27. J.E.G. Gonzalez and J.C. Mirza-Rosca, *J. Electroanal. Chem.* **471** (1999) 109.
28. M.A. Khan, R.L. Williams and D.F. Williams, *Biomaterials* **20** (1999) 631.
29. A. Husain and G. Singh, *Indian J. Technol.* **31** (1993) 660.
30. Z.Y. Jiang, Y.T. Wang, Q. Yu and S.Y. Huang, *Corros. Sci.* **37** (1995) 1245.
31. N.V. Shel, L.E. Tsygankova and V.I. Vigdorovich, *Prot. Met.* **33** (1997) 141.
32. M.M.A. Gad, K.E. Mohamed and A.A. El-Sayed, *J. Mater. Sci. Technol.* **16** (2000) 45.
33. J.P. Frayret, A. Caprani, H. Luc and F. Priem, *Corrosion* **40** (1984) 14.
34. J.P. Frayret, A. Caprani, T. Jaszay and F. Priem, *Corrosion* **41** (1985) 656.
35. V.B. Singh and M.A. Hosseini, *Indian J. Technol.* **32** (1994) 287.
36. A. Rauscher and Z. Lukacs, *Werkst. Korros.* **39** (1988) 280.
37. V.B. Singh and M.A. Hosseini, *Corros. Sci.* **34** (1993) 1723.
38. V.B. Singh and M.A. Hosseini, *J. Appl. Electrochem.* **24** (1994) 250.
39. '1985 Annual Book of ASTM Standards', Vol. 03.01, ASTM, Philadelphia, PA, (1985).
40. M. Pourbaix, 'Atlas of Electrochemical Equilibria in Aqueous Solutions', Vol. 1, Pergamon Press, New York, (1966), p. 213.
41. A. Robin, H.R.Z. Sandim and J.L. Rosa, *Corros. Sci.* **41** (1999) 1333.